Mutations in Complex I Assembly Factor *TMEM126B* Result in Muscle Weakness and Isolated Complex I Deficiency

Laura Sánchez-Caballero,[1,7] Benedetta Ruzzenente,[2,7] Lucas Bianchi,[2] Zahra Assouline,[3] Giulia Barcia,[3] Metodi D. Metodiev,[2] Marlène Rio,[3] Benoît Funalot,[4] Mariël A.M. van den Brand,[1] Sergio Guerrero-Castillo,[1] Joery P. Molenaar,[5] David Koolen,[6] Ulrich Brandt,[1] Richard J. Rodenburg,[1] Leo G. Nijtmans,[1,7,*] and Agnès Rötig[2,7,*]

Mitochondrial complex I deficiency results in a plethora of often severe clinical phenotypes manifesting in early childhood. Here, we report on three complex-I-deficient adult subjects with relatively mild clinical symptoms, including isolated, progressive exercise-induced myalgia and exercise intolerance but with normal later development. Exome sequencing and targeted exome sequencing revealed compound-heterozygous mutations in *TMEM126B*, encoding a complex I assembly factor. Further biochemical analysis of subject fibroblasts revealed a severe complex I deficiency caused by defective assembly. Lentiviral complementation with the wild-type cDNA restored the complex I deficiency, demonstrating the pathogenic nature of these mutations. Further complexome analysis of one subject indicated that the complex I assembly defect occurred during assembly of its membrane module. Our results show that TMEM126B defects can lead to complex I deficiencies and, interestingly, that symptoms can occur only after exercise.

Isolated complex I (CI) deficiency is the most frequent cause of respiratory-chain defects in childhood and accounts for various clinical presentations. Neurological presentations are often observed, given that numerous individuals present with Leigh syndrome (MIM: 256000), Leber hereditary optic neuropathy (MIM: 535000), and mitochondrial encephalomyopathy, lactic acidosis, and stroke-like episodes (MIM: 540000). In addition, numerous other clinical presentations combining hypotonia, developmental delay, seizures, cardiomyopathy, optic atrophy or retinopathy, and other organ involvement have been reported.[1–3] Mitochondrial CI is the largest enzyme of the oxidative phosphorylation (OXPHOS) system.[4,5] It is embedded in the inner mitochondrial membrane[6,7] and is composed of three different functional and structural modules.[4] The entry point of electrons is the NADH dehydrogenase module (N module), which contains a flavin mononucleotide where NADH is oxidized, after which the electrons are transferred along a chain of iron-sulfur clusters to the Q module, where ubiquinone is subsequently reduced. For every two electrons transferred from NADH to ubiquinone, four protons are ejected from the mitochondrial matrix via the proton-pumping module (P module).[4,8–11] It has been established that the assembly of CI in vivo is a stepwise process in which different preassembled modules are combined into the mature holoenzyme.[12,13] CI deficiencies are associated with mutations in mitochondrial and nuclear genes encoding structural subunits but also in nuclear genes encoding CI-specific assembly factors.[1] Interestingly, most of these assembly factors were first discovered in individuals with a mitochondrial CI deficiency.[14–24] Only a few CI assembly factors have been identified by functional studies in normal cellular models.[25–31] One of these is TMEM126B, a mitochondrial transmembrane protein. Deficiency of this protein has been shown to reduce the total amount of CI in a cellular model system.[25,29] Furthermore, it has been shown that TMEM126B forms a complex with other assembly factors: NDUFAF1, ACAD9, and Ecsit.[25,29] We identified *TMEM126B* (MIM: 615533) mutations in three unrelated subjects with exercise intolerance, hyperlactatemia, and isolated CI deficiency.

Subject 1, a 38-year-old man of European descent, was born to non-consanguineous healthy parents. He had progressive muscle complaints from the age of 38 years onward and was referred to our clinic with progressive exercise-induced myalgia (most predominantly in his calves). Resting relieved the symptoms, and there was no second-wind phenomenon. Fasting did not affect the myalgia, and signs of rhabdomyolysis were absent. He also suffered from excessive daily fatigue. His early development had been normal, and he reported normal functional abilities. Neurological examination and electromyography were normal. Laboratory investigations revealed hyperlactatemia (2.9–4.8 mmol/L; control values < 2 mmol/L) and hyperalaninemia (772 μmol/L; control values = 150–450 μmol/L) and a blood pH of 7.25 at rest. Other laboratory tests, including creatine kinase, were normal. A

[1]Radboud Center for Mitochondrial Medicine, Department of Pediatrics, Radboud University Medical Center, Geert Grooteplein Zuid 10, 6525 GA Nijmegen, the Netherlands; [2]INSERM U1163, Université Paris Descartes – Sorbonne Paris Cité, Institut Imagine, 75015 Paris, France; [3]Departments of Pediatrics and Genetics, Hôpital Necker-Enfants Malades, 75015 Paris, France; [4]Department of Genetics, Hôpital Henri Mondor, 94010 Créteil, France; [5]Department of Neurology, Radboud University Medical Center, Geert Grooteplein Zuid 10, 6525 GA Nijmegen, the Netherlands; [6]Department of Human Genetics, Radboud Institute for Molecular Life Sciences, Radboud University Medical Center, 6500 HB Nijmegen, the Netherlands
[7]These authors contributed equally to this work
*Correspondence: leo.nijtmans@radboudumc.nl (L.G.N.), agnes.rotig@inserm.fr (A.R.)
http://dx.doi.org/10.1016/j.ajhg.2016.05.022.

muscle biopsy showed no abnormalities with standard immunohistochemical staining techniques, including Gomori trichrome and oxidative staining. However, electron microscopy showed several abnormalities indicating mitochondrial dysfunction: most mitochondria were swollen (some were giant), most of the mitochondria were surrounded by lipid droplets, and a few mitochondria showed crystalline inclusions (Figure 1A). Activity of respiratory-chain enzymes indicated a severe CI deficiency in muscle and fibroblasts (Table 1).

Subject 2, a 30-year-old woman of European descent, was born to healthy unrelated parents after a normal pregnancy and delivery. Her younger brother is healthy. Psychomotor development was normal. From the age of 9 years, she experienced exercise intolerance, manifested by premature exertional muscle fatigue, myalgia, dyspnea, and cardiac palpitations for relatively intense efforts, such as running, but not for moderate efforts. Indeed, her walking distance was not markedly reduced. Levels of blood creatine kinase were always normal at rest and during acute episodes. At the age of 23 years, she was admitted for investigations. Height and weight were 1.61 m and 49 kg, respectively. She had a normal physical appearance but had mild proximal muscle weakness at examination. Electrocardiography and echocardiography were normal. Ophthalmological examination was completely normal and showed no sign of retinitis pigmentosa at fundoscopy or optic atrophy. Metabolic investigations showed hyperlactatemia (7 mmol/L; control values < 2 mmol/L) and hyperalaninemia (1,120 μmol/L; control values $= 274 \pm 50$ μmol/L) and an increased lactate/pyruvate ratio (33; control values = 10–20). Measurement of urine organic acids showed elevated lactate levels (8,000 μmol/mmol creatinine; control values < 84 μmol/mmol creatinine). CI activity was severely reduced in muscle mitochondria (Table 1).

Subject 3, a 22-year-old man of European descent, was the first child born to healthy unrelated parents after a normal pregnancy and delivery. His younger brother is healthy. He was able to walk at 18 months. He was noted to have proximal muscle weakness at 3 years of age. He had lifelong exercise intolerance marked by myalgia followed by vomiting. Nevertheless, he was reported to have normal physical activity. At 14 years of age, neurological examination was normal. His height and weight were 1.49 m and 37.7 kg, respectively. Metabolic investigations showed permanent hyperlactacidemia (2.8–7.4 mmol/L), elevated lactate/pyruvate ratios (21–32), hyperalaninemia (702 μmol/L; normal range $= 274 \pm 50$ μmol/L), and elevated lactate levels in urine (2,775 μmol/mmol creatinine; control values < 84 μmol/mmol creatinine). Ophthalmological and cardiac examination was normal. A severe CI deficiency was observed in muscle (Table 1).

Informed consent for diagnostic and research studies was obtained for all subjects in accordance with the Declaration of Helsinki protocols and approved by local institutional review boards in Nijmegen and Paris.

To identify the disease-causing genetic defect, we performed whole-exome sequencing of subject 1. Putative pathogenic variants were selected after filtering against known SNPs in dbSNP, 1000 Genomes, the National Heart, Lung, and Blood Institute (NHLBI) Exome Sequencing Project Exome Variant Server, intergenic variants, and an in-house variant database. This revealed two heterozygous variants in *TMEM126B* (GenBank: NM_018480.4): c.635G>T (p.Gly212Val) and c.397G>A (p.Asp133Asn) (Figures 1B–1D). These variants were confirmed by Sanger sequencing. Segregation analysis revealed that the mother of subject 1 carries the c.635G>T variant and the father carries the c.397G>A variant.

The genetic defect in subject 2 was identified by targeted exome sequencing of a panel of 215 genes, including the known genes for mitochondrial disorders and genes of CI subunits and assembly factors. This revealed two *TMEM126B* heterozygous variants that were confirmed by Sanger sequencing (c.635G>T inherited from the mother and c.208C>T [p.Gln70*] inherited from the father; Figures 1B–1D). Considering the similar clinical presentation of subjects 2 and 3, we performed Sanger sequencing of *TMEM126B* for subject 3 and detected two *TMEM126B* heterozygous variants (c.635G>T and c.397G>A, inherited from the mother and father, respectively; Figures 1B–1D).

The c.397G>A and c.635G>T variants are present in the European population with a very low allele frequency (Table 2). The p.Gly212Val change was predicted to be deleterious by three different prediction software packages, namely SIFT, MutationTaster, and PolyPhen-2 (Table 2). The c.397G>A (rs573006534) variant is predicted to lead to the loss of the 3′ splice site of exon 3. Sanger sequencing of RT-PCR products encompassing exon 3 revealed two superimposed sequence traces (Figure 1D), suggesting that an alternative splice site located at position 293–296 was used instead, which generated a truncated cDNA lacking 104 bp from exon 3 (Figure 1E). This truncated transcript most likely had reduced stability given that sequencing of exon 5 from total cDNA predominantly detected the c.635G>T variant (Figure 1D). Using RT-PCR, we amplified three distinct *TMEM126B* transcripts—*TMEM126B.1* (GenBank: NM_018480.4), *TMEM126B.2* (GenBank: NM_001193537.2), and *TMEM126B.5* (GenBank: NM_001256546.1)—the first and last of which have been previously reported. Transcript 5 is generated by an alternative start codon downstream of the initiating methionine of transcript 1, whereas transcript 2 is a result of alternative splicing (Figure 1B). All isoforms have identical exons 3–5. Thus, the identified mutations, which localize in exons 3 and 5, affect all three *TMEM126B* isoforms. Therefore, the three subjects have the same c.635G>T mutation resulting in p.Gly212Val from the maternal allele and either a splice mutation resulting in an unstable transcript or a premature stop codon from the paternal allele. The low allelic frequencies of c.397G>A and c.635G>T, the absence of

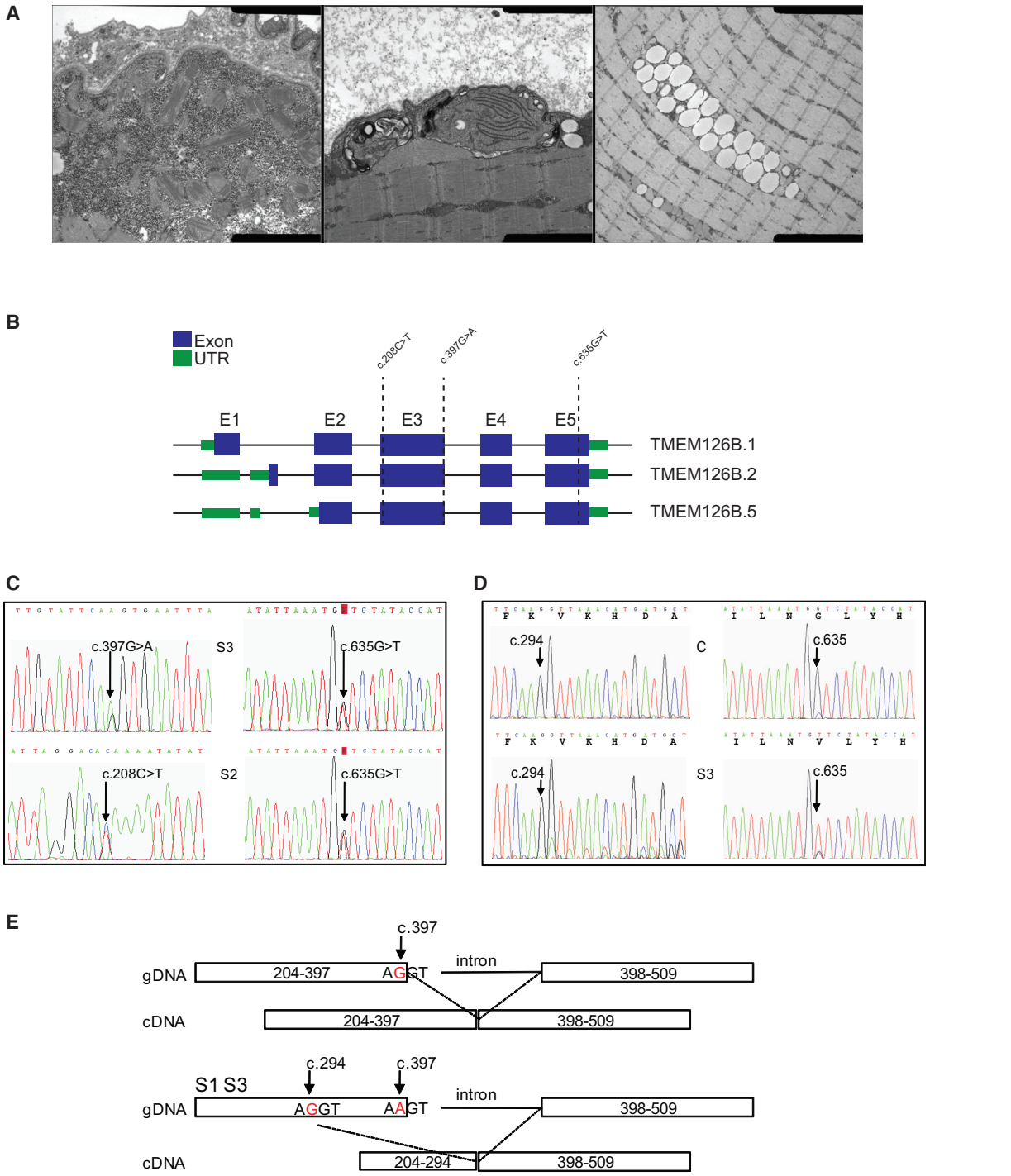

Figure 1. Mutations in *TMEM126B* Are Associated with Mitochondrial Dysfunction
(A) Electron micrographs of skeletal muscle sections from subject 1 show a mitochondrion with cristalline inclusions (left), a giant mitochondrion (center), and mitochondria surrounded by lipid droplets (right).
(B) Exon-intron organization of *TMEM126B* depicts the three human cDNA isoforms (*TMEM126B.1*, *TMEM126B.2*, and *TMEM126B.5*). The positions of the *TMEM126B* variants identified in the subjects are indicated.
(C) Sequence analysis of *TMEM126B* of subjects 1–3 (S1–S3). The arrows indicate the mutations.
(D) Sequence analysis of RT-PCR of *TMEM126B* exons 3–5 shows in subject 3 (S3) a heterozygous exon 3 deletion starting at c.295 underneath the normal allele (left) and a much lower amount of the c.635G>T variation in exon 5 in subject 3 than in the control (right).
(E) Partial structure of *TMEM126B* (gDNA) and cDNA. The exon-intron junctions, as well as the consensus splice sites, are presented. c.294 indicates the putative consensus splice site (AGGT) that could have been used as new splice site in subjects 1 and 3.

Table 1. Respiratory-Chain Activities in Muscle Mitochondria, Muscle Homogenate, and Fibroblasts

	Muscle Mitochondria				Muscle Homogenate		Fibroblasts					
	S1	C	S2	C	S3	C	S1	C	S2	C	S3	C
CI/CS	0.03[a]	0.47–1.54	0.02[a]	0.14–0.19	0.02[a]	0.12–0.22	0.05[a]	0.16–0.60	ND	0.11–0.17	ND	0.12–0.26
CII/CS	0.21	0.13–0.35	0.28	0.23–0.29	0.26	0.24–0.38	0.53	0.34–0.89	0.36	0.24–0.30	0.31	0.25–0.34
CIII/CS	0.84	0.70–1.76	5.05	3.44–4.66	ND	2.29–3.64	0.87	0.57–1.38	2.03	2.37–3.06	3.30	2.24–2.97
CIV/CS	1.01	0.47–1.84	2.49	1.65–2.19	1.42	1.24–1.97	0.43	0.29–0.95	0.86	1.13–1.48	1.70	1.14–1.54
CV/CS	ND	ND	1.40	0.66–0.94	ND	0.46–0.97	0.72	0.20–0.82	0.20	0.21–0.29	ND	0.23–0.33

Abbreviations are as follows: CI–CV, complexes I–V, respectively; CS, citrate synthase; S1–S3, subjects S1–S3, respectively; C, control values; and ND, not done.
[a]Abnormal values.

c.208C>T in SNP databases, the compound-heterozygous state of the *TMEM126B* variations, and the recurrence of these mutations in three independent subjects with a similar clinical phenotype and an isolated CI deficiency are highly suggestive of a pathogenic effect on CI activity.

Blue native PAGE (BN-PAGE) analyses revealed a marked decrease in fully assembled CI in cultured skin fibroblasts of the three subjects (Figures 2A and 2B), consistent with the isolated CI defect detected in muscle biopsies. Although the other OXPHOS complexes were all present at similar levels between subjects and control fibroblasts, we detected a mild increase in the $CIII_2$-CIV supercomplex, suggesting that supercomplex composition undergoes a general rearrangement as a result of the decrease in CI levels. To further investigate this, we solubilized mitoplasts isolated from fibroblasts of subject 1 and control cells in digitonin, a detergent that preserves the high-molecular-weight respiratory-chain supercomplexes. The amount of CI-containing supercomplexes, detected either by an in-gel enzyme assay (IGA) or by immunoblotting, was lower in subject 1 than in control cells (Figure 2C). Similarly, we found a decreased level of CI-$CIII_2$-CIV_n supercomplexes visualized with specific antibodies for complexes III and IV (Figure 2C). On the other hand, supercomplex CIII-CIV and monomeric CIV were found to be slightly increased in subject 1 fibroblasts (Figure 2C). Consistent with these results, immunoblot analyses of total protein extracts from subjects 2 and 3 and control fibroblasts revealed decreased levels of the CI subunit NDUFB8 for subject 2 and increased steady-state levels of subunits CIII and CIV, UQCR2, and COX1 for subject 3 (Figure 2D).

Table 2. *TMEM126B* Variations Identified in Subjects S1–S3 and Predicted Consequences

	Subjects		
	S2	S1 and S3	S1, S2, and S3
Nucleotide change	c.208C>T	c.397G>A	c.635G>T
Amino acid change	p.Gln70*	p.Asp133Asn	p.Gly212Val
SIFT	NA	tolerated (score = 0.12)	deleterious (score = 0.03)
MutationTaster	NA	disease causing (p value = 1)	disease causing (p value = 0.946)
PolyPhen-2	NA	benign (score = 0.084)	probably damaging (score = 0.995)
Predicted change at donor site 1 bp downstream	NA	−56.8%	NA
MaxEnt	NA	−77.6%	NA
NNSPLICE	NA	−80.5%	NA
Human Splicing Finder	NA	−12.2%	NA
dbSNP (MAF/minor allele count)	none	rs573006534 (<0.01/1)	rs141542003 (unknown)
ClinVar	–	–	–
ExAC allele frequency	none	A = 0.0089%	T = 0.13%
NHLBI EVS	none	–	T = 16/G = 8,582 (European American)
			T = 0/G = 4,406 (African American)

The effect of the variations on the protein was predicted by Alamut software including SIFT, MutationTaster, and PolyPhen-2. The frequency of the variations in dbSNP, ClinVar, the Exome Aggregation Consortium (ExAC) Browser, and the NHLBI Exome Variant Server (EVS) are presented. The predicted splicing modifications were determined by Alamut software including MaxEnt, NNSPLICE, and the Human Splicing Finder. The *TEM126B* reference sequence is GenBank: NM_001193537. The following abbreviation is used: NA, not appropriate.

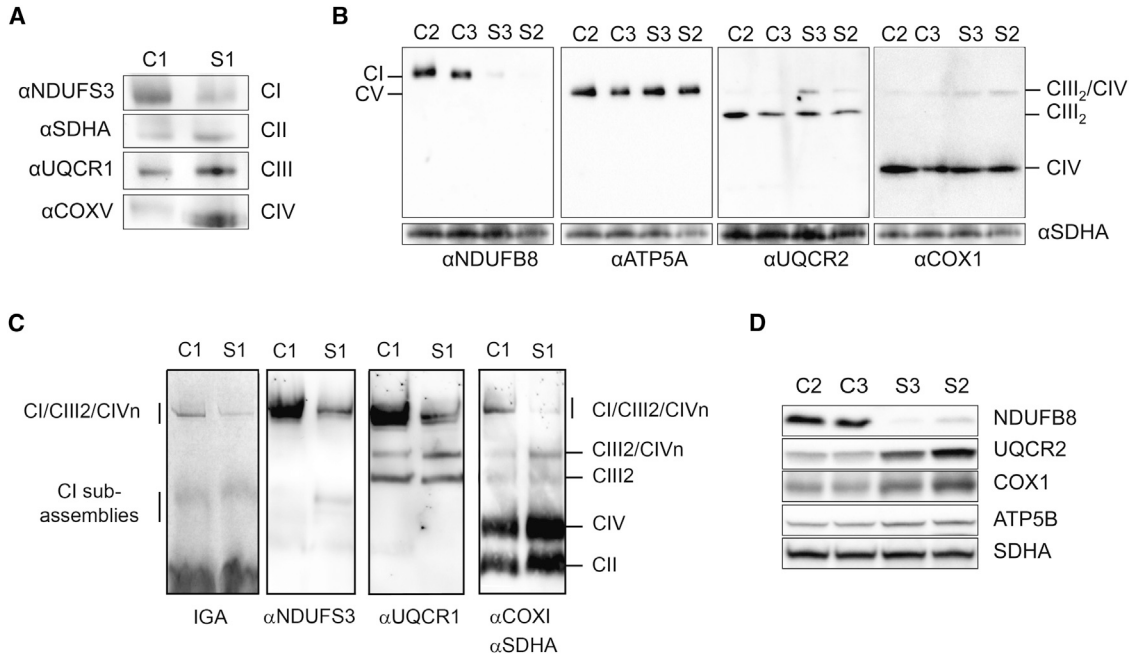

Figure 2. Isolated CI Deficiency in Subjects with *TMEM126B* Variants

(A and B) BN-PAGE analysis revealed an isolated CI assembly defect in fibroblasts from subject S1 (A) and subjects S2 and S3 (B). Mitoplasts (20 or 80 μg) isolated from control and subject fibroblasts were solubilized with 1% DDM, fractionated through 3%–12% native gels, and transferred to either PVDF or Protran nitrocellulose membranes. The individual complexes were identified with specific antibodies.

(C) Mitoplasts from a control (C1) and subject 1 (S1) were solubilized in 2% digitonin and subjected to BN-PAGE as in (A). Supramolecular organization of the respiratory-chain complexes was detected by IGA for CI or immunoblotting with specific antibodies.

(D) SDS-PAGE analysis of the steady-state levels of OXPHOS proteins. Total protein cell extracts (20 μg) from control (C2 and C3) and subject (S2 and S3) fibroblasts were fractionated through 12% polyacrylamide gels and transferred to PVDF membranes. Individual OXPHOS proteins were detected with specific antibodies. SDHA was used as a loading control.

Because TMEM126B had been recently reported to function as an assembly factor for CI,[29] we proceeded to study in more detail the assembly defect of CI in subjects' fibroblasts. The decreased level of fully assembled CI was accompanied by an accumulation of subassembled intermediates in all three subjects (Figures 3A and 3B). These intermediates belong to the Q and P modules, given that they are detected by antibodies against NDUFS3 and NDUFA13, respectively, which localize in these modules. Using two-dimensional BN-SDS-PAGE (BN-PAGE followed by SDS-PAGE), further characterization of the subassembled intermediates in subject 1 fibroblasts revealed a profound reduction in the molecular weight of the NDUFS3-containing module (Figure 3C). Similarly, we detected an accumulation of ACAD9, an assembly factor of the CI membrane arm, at a lower molecular level in subject 1 fibroblasts (Figure 3C). These results indicate that the assembly of the individual CI functional modules is impaired in subjects carrying *TMEM126B* mutations.

Interestingly, NDUFAF1 and ACAD9, assembly factors acting at the level of the CI membrane arm where TMEM126B is expected to interact,[25,29,32] showed increased steady-state levels in protein extracts from subject 1 fibroblasts. In fibroblasts of subjects 2 and 3, CI subunits NDUFS3, NDUFB8, and NDUFA9 were decreased, which is in line with the decreased assembly of complex I (Figures 3D and 3E).

In order to confirm that the CI deficiency observed in the three subjects is indeed due to the *TMEM126B* variants, we performed functional complementation studies by using lentiviral expression of the different wild-type *TMEM126B* isoforms with a 3′ FLAG tag. Lentiviral expression of the three isoforms in fibroblasts from subjects 3 (Figure 3F) and 2 (data not shown) partially restored CI assembly and resulted in increased steady-state levels of NDUFB8 and NDUFA13, whereas CI subassemblies were reduced in the complemented fibroblasts. Similarly, expression of *TMEM126B.5* in subject 1 fibroblasts partially restored assembly (Figure 3G) and in vitro activity of CI (Table S1). These results demonstrate the causal role of *TMEM126B* mutations in the CI assembly defect observed in the three subjects.

To obtain more in-depth information concerning the disturbed CI assembly process, we performed complexome profiling[29,33] in control, subject 1, and complemented subject 1 fibroblasts. This mass-spectrometry-based approach provides unbiased insight into the amount and composition of complexes, including CI subassemblies. This analysis led to several observations. We could demonstrate a clear improvement in CI assembly, whereby more mature CI and fewer subassemblies accumulated in the complemented cells than in the subjects' cells (Figure 4A). The only TMEM126B peptide detectable by mass spectrometry

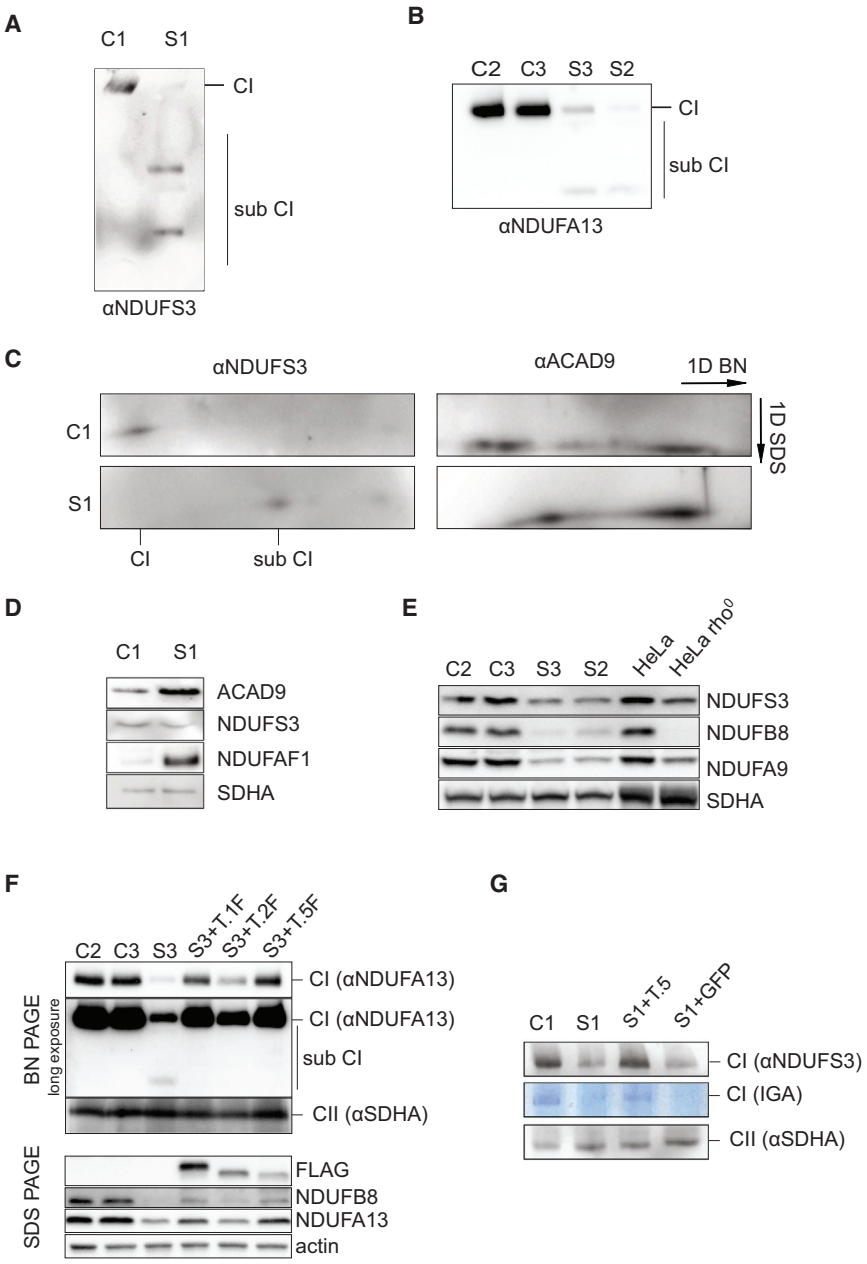

Figure 3. CI Assembly Defects in Subject Fibroblasts Were Restored after Lentiviral Expression of Wild-Type *TMEM126B*

(A and B) Mitoplasts isolated from control (C1 and C3) and subject (S1–S3) fibroblasts were solubilized with DDM and analyzed as in Figures 2A and 2B. NDUFS3 and NDUFA13 in CI subassemblies were detected with specific antibodies.

(C) Mitochondria isolated from control (C1) and subject (S1) fibroblasts were solubilized in 2% DDM, subjected to two-dimensional BN-SDS-PAGE analysis, and transferred onto Protran nitrocellulose membranes. NDUFS3 and ACAD9 were detected with specific antisera.

(D) Steady-state levels of the CI structural protein NDUFS3 and the CI assembly factors ACAD9 and NDUFAF1 were determined by SDS-PAGE analysis and immunoblotting of total cell extracts (40 μg) from control (C1) and subject (S1) fibroblasts with specific antibodies. SDHA was used as a loading control.

(E) Steady-state levels of structural CI proteins were determined by SDS-PAGE and immunoblotting of total cell extracts (30 μg) from control (C2 and C3) and subject (S2 and S3) fibroblasts, HeLa cells, and HeLa rho° cells with specific antibodies. SDHA was used as a loading control.

(F) Subject 3 fibroblasts were transduced with lentiviral particles expressing wild-type *TMEM126B.1*, *TMEM126B.2*, or *TMEM126B.5* fused to a 3′ FLAG tag (T.1F, T.2F, or T.5F, respectively). Mitoplasts (20 μg, upper panel) were analyzed by BN-PAGE as in Figures 2A and 2B. CI assembly was partially restored by expression of the three isoforms. SDS-PAGE analysis (lower panel) of total cell protein extracts (20 μg) was performed as in Figure 2D and showed expression of all three *TMEM126B* isoforms and partial restoration of NDUFA13 and NDUFB8 steady-state levels. Actin was used as a loading control.

(G) Fibroblasts from subject 1 (S1) were transduced with lentiviral particles expressing wild-type *TMEM126B*.5 (T.5) or GFP. CI assembly and activity were analyzed by BN-PAGE followed by immunoblotting or IGA.

was not present in isoform 5. Therefore, by complexome profiling, we could monitor only isoforms 1 and 2, which were almost undetectable in the subject 1 fibroblasts (Figure 4B). This also meant that we could not observe an increase in TMEM126B in the fibroblasts complemented with isoform 5. Still, the accumulation of higher-molecular-mass versions of the assembly-factor complexes observed in subject 1 fibroblasts was largely reversed, indirectly indicating successful complementation. In addition, we observed accumulation of CI subassemblies of the ubiquinone binding part, a decrease in the NADH binding part, and a disturbed proton-pumping part in subject 1 fibroblasts (Figure 4A), consistent with our immunoblot data (see Figure 3 above). TMEM126B was decreased in subject 1 fibroblasts but present together with ACAD9, Ecsit, and NDUFAF1 in control fibroblasts (Figure 4B). Interestingly, its paralog TMEM126A was detectable in mitochondrial complexes only in the fibroblasts of the subject with a defect in TMEM126B. Moreover, it seemed to co-migrate with the CI assembly factors ACAD9 and NDUFAF1, whereas in control fibroblasts, TMEM126A was not associated with any mitochondrial complex. This observation of TMEM126A co-migrating with CI assembly factors has been reported before in HEK293 cells.[34] *TMEM126B* comes from a duplication of its ancestor *TMEM126A* (MIM: 612988), and they share 85% similarity in their nucleotide sequences. TMEM126B is evolutionary one of the most recent CI assembly factors and is only present in mammals.

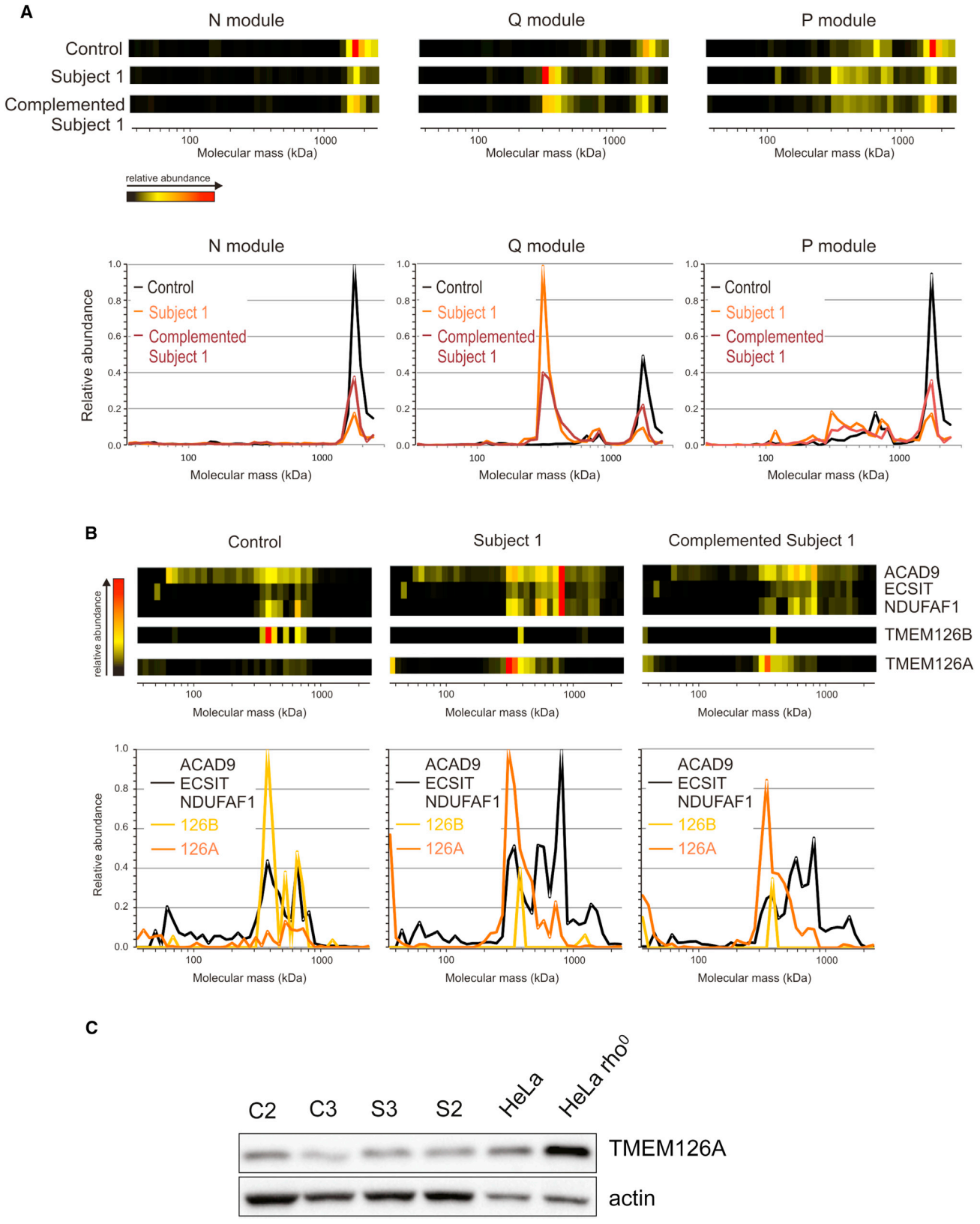

Figure 4. Complexome Profiling of Control, Subject, and Complemented Subject Fibroblasts
(A and B) Heatmaps (top) and migration profiles (bottom) obtained by complexome profiling of mitochondria isolated from control (C1), subject 1, and complemented subject 1 fibroblasts. (A) CI subunits belonging to N, Q, and P modules. (B) CI assembly factors (ACAD9, ECSIT, NDUFAF1, and TMEM126B) and TMEM126A.
(C) Steady-state levels of TMEM126A were determined by SDS-PAGE analysis and immunoblotting of total cell extracts (30 μg) from control (C2 and C3) and subject (S2 and S3) fibroblasts, HeLa cells, and HeLa rho° cells with specific antibodies. Actin was used as a loading control.

The replacement of TMEM126B with its paralog TMEM126A in the CI assembly process in the subjects presented here might suggest a compensatory mechanism. Analyses of the steady-state levels of TMEM126A showed that the protein was unchanged between control fibroblasts and those from subjects 2 and 3, whereas it was found upregulated in rho° HeLa cells, in which expression of the seven genes encoding hydrophobic core subunits is abolished (Figure 4C). Interestingly, homozygous mutations in *TMEM126A* have been associated with isolated optic atrophy.[35] Nevertheless, the role of TMEM126A in CI assembly has not been demonstrated and requires further research.

In conclusion, by using whole-exome sequencing and targeted sequencing, we found mutations in the gene encoding the CI assembly factor TMEM126B in three subjects. Using any of the wild-type *TMEM126B* isoforms to restore the biochemical defects establishes that the TMEM126B defects are disease causing in these subjects. The clinical phenotype, compared with other complex I defects, is relatively mild. In-depth analysis using complexome profiling allows us to pinpoint the defect to a specific stage of the CI assembly process.

Supplemental Data

Supplemental Data include one table and can be found with this article online at http://dx.doi.org/10.1016/j.ajhg.2016.05.022.

Acknowledgments

We would like to acknowledge the Genome Technology Center at the Radboud UMC and BGI Copenhagen for providing the exome sequencing service. This work was partially funded by the European Commission (FP7-PEOPLE-ITN. GA. 317433), by the Association Française contre les Myopathies (MNM 2012 no. 15740), and by the E-Rare project GENOMIT (01GM1207).

Received: March 4, 2016
Accepted: May 17, 2016
Published: June 30, 2016

Web Resources

1000 Genomes, http://www.1000genomes.org/
Alamut Interpretation Software 2.0, http://alamut.interactivebiosoftware.com
ClinVar, http://www.ncbi.nlm.nih.gov/clinvar/
dbSNP, http://www.ncbi.nlm.nih.gov/SNP/
ExAC Browser, http://exac.broadinstitute.org/
NHLBI Exome Sequencing Project (ESP) Exome Variant Server, http://evs.gs.washington.edu/EVS/
OMIM, http://www.omim.org/
RefSeq, http://www.ncbi.nlm.nih.gov/refseq/

References

1. Nouws, J., Nijtmans, L.G., Smeitink, J.A., and Vogel, R.O. (2012). Assembly factors as a new class of disease genes for mitochondrial complex I deficiency: cause, pathology and treatment options. Brain *135*, 12–22.
2. Koene, S., Rodenburg, R.J., van der Knaap, M.S., Willemsen, M.A., Sperl, W., Laugel, V., Ostergaard, E., Tarnopolsky, M., Martin, M.A., Nesbitt, V., et al. (2012). Natural disease course and genotype-phenotype correlations in Complex I deficiency caused by nuclear gene defects: what we learned from 130 cases. J. Inherit. Metab. Dis. *35*, 737–747.
3. Fassone, E., and Rahman, S. (2012). Complex I deficiency: clinical features, biochemistry and molecular genetics. J. Med. Genet. *49*, 578–590.
4. Brandt, U. (2006). Energy converting NADH:quinone oxidoreductase (complex I). Annu. Rev. Biochem. *75*, 69–92.
5. Hirst, J. (2013). Mitochondrial complex I. Annu. Rev. Biochem. *82*, 551–575.
6. Vinothkumar, K.R., Zhu, J., and Hirst, J. (2014). Architecture of mammalian respiratory complex I. Nature *515*, 80–84.
7. Zickermann, V., Wirth, C., Nasiri, H., Siegmund, K., Schwalbe, H., Hunte, C., and Brandt, U. (2015). Structural biology. Mechanistic insight from the crystal structure of mitochondrial complex I. Science *347*, 44–49.
8. Baradaran, R., Berrisford, J.M., Minhas, G.S., and Sazanov, L.A. (2013). Crystal structure of the entire respiratory complex I. Nature *494*, 443–448.
9. Hirst, J., Carroll, J., Fearnley, I.M., Shannon, R.J., and Walker, J.E. (2003). The nuclear encoded subunits of complex I from bovine heart mitochondria. Biochim. Biophys. Acta *1604*, 135–150.
10. Walker, J.E. (1992). The NADH:ubiquinone oxidoreductase (complex I) of respiratory chains. Q. Rev. Biophys. *25*, 253–324.
11. Carroll, J., Fearnley, I.M., Shannon, R.J., Hirst, J., and Walker, J.E. (2003). Analysis of the subunit composition of complex I from bovine heart mitochondria. Mol. Cell. Proteomics *2*, 117–126.
12. Ugalde, C., Vogel, R., Huijbens, R., Van Den Heuvel, B., Smeitink, J., and Nijtmans, L. (2004). Human mitochondrial complex I assembles through the combination of evolutionary conserved modules: a framework to interpret complex I deficiencies. Hum. Mol. Genet. *13*, 2461–2472.
13. Vogel, R., Nijtmans, L., Ugalde, C., van den Heuvel, L., and Smeitink, J. (2004). Complex I assembly: a puzzling problem. Curr. Opin. Neurol. *17*, 179–186.
14. Kevelam, S.H., Rodenburg, R.J., Wolf, N.I., Ferreira, P., Lunsing, R.J., Nijtmans, L.G., Mitchell, A., Arroyo, H.A., Rating, D., Vanderver, A., et al. (2013). NUBPL mutations in patients with complex I deficiency and a distinct MRI pattern. Neurology *80*, 1577–1583.
15. Tenisch, E.V., Lebre, A.S., Grévent, D., de Lonlay, P., Rio, M., Zilbovicius, M., Funalot, B., Desguerre, I., Brunelle, F., Rötig, A., et al. (2012). Massive and exclusive pontocerebellar damage in mitochondrial disease and NUBPL mutations. Neurology *79*, 391.
16. Tucker, E.J., Mimaki, M., Compton, A.G., McKenzie, M., Ryan, M.T., and Thorburn, D.R. (2012). Next-generation sequencing in molecular diagnosis: NUBPL mutations highlight the challenges of variant detection and interpretation. Hum. Mutat. *33*, 411–418.
17. Ogilvie, I., Kennaway, N.G., and Shoubridge, E.A. (2005). A molecular chaperone for mitochondrial complex I assembly is mutated in a progressive encephalopathy. J. Clin. Invest. *115*, 2784–2792.

18. Saada, A., Vogel, R.O., Hoefs, S.J., van den Brand, M.A., Wessels, H.J., Willems, P.H., Venselaar, H., Shaag, A., Barghuti, F., Reish, O., et al. (2009). Mutations in NDUFAF3 (C3ORF60), encoding an NDUFAF4 (C6ORF66)-interacting complex I assembly protein, cause fatal neonatal mitochondrial disease. Am. J. Hum. Genet. *84*, 718–727.
19. Saada, A., Edvardson, S., Rapoport, M., Shaag, A., Amry, K., Miller, C., Lorberboum-Galski, H., and Elpeleg, O. (2008). C6ORF66 is an assembly factor of mitochondrial complex I. Am. J. Hum. Genet. *82*, 32–38.
20. Fassone, E., Duncan, A.J., Taanman, J.W., Pagnamenta, A.T., Sadowski, M.I., Holand, T., Qasim, W., Rutland, P., Calvo, S.E., Mootha, V.K., et al. (2010). FOXRED1, encoding an FAD-dependent oxidoreductase complex-I-specific molecular chaperone, is mutated in infantile-onset mitochondrial encephalopathy. Hum. Mol. Genet. *19*, 4837–4847.
21. Sugiana, C., Pagliarini, D.J., McKenzie, M., Kirby, D.M., Salemi, R., Abu-Amero, K.K., Dahl, H.H., Hutchison, W.M., Vascotto, K.A., Smith, S.M., et al. (2008). Mutation of C20orf7 disrupts complex I assembly and causes lethal neonatal mitochondrial disease. Am. J. Hum. Genet. *83*, 468–478.
22. Gerards, M., Sluiter, W., van den Bosch, B.J., de Wit, L.E., Calis, C.M., Frentzen, M., Akbari, H., Schoonderwoerd, K., Scholte, H.R., Jongbloed, R.J., et al. (2010). Defective complex I assembly due to C20orf7 mutations as a new cause of Leigh syndrome. J. Med. Genet. *47*, 507–512.
23. Dunning, C.J., McKenzie, M., Sugiana, C., Lazarou, M., Silke, J., Connelly, A., Fletcher, J.M., Kirby, D.M., Thorburn, D.R., and Ryan, M.T. (2007). Human CIA30 is involved in the early assembly of mitochondrial complex I and mutations in its gene cause disease. EMBO J. *26*, 3227–3237.
24. Fassone, E., Taanman, J.W., Hargreaves, I.P., Sebire, N.J., Cleary, M.A., Burch, M., and Rahman, S. (2011). Mutations in the mitochondrial complex I assembly factor NDUFAF1 cause fatal infantile hypertrophic cardiomyopathy. J. Med. Genet. *48*, 691–697.
25. Andrews, B., Carroll, J., Ding, S., Fearnley, I.M., and Walker, J.E. (2013). Assembly factors for the membrane arm of human complex I. Proc. Natl. Acad. Sci. USA *110*, 18934–18939.
26. Janssen, R., Smeitink, J., Smeets, R., and van Den Heuvel, L. (2002). CIA30 complex I assembly factor: a candidate for human complex I deficiency? Hum. Genet. *110*, 264–270.
27. Vogel, R.O., Janssen, R.J., van den Brand, M.A., Dieteren, C.E., Verkaart, S., Koopman, W.J., Willems, P.H., Pluk, W., van den Heuvel, L.P., Smeitink, J.A., and Nijtmans, L.G. (2007). Cytosolic signaling protein Ecsit also localizes to mitochondria where it interacts with chaperone NDUFAF1 and functions in complex I assembly. Genes Dev. *21*, 615–624.
28. Nouws, J., Nijtmans, L., Houten, S.M., van den Brand, M., Huynen, M., Venselaar, H., Hoefs, S., Gloerich, J., Kronick, J., Hutchin, T., et al. (2010). Acyl-CoA dehydrogenase 9 is required for the biogenesis of oxidative phosphorylation complex I. Cell Metab. *12*, 283–294.
29. Heide, H., Bleier, L., Steger, M., Ackermann, J., Dröse, S., Schwamb, B., Zörnig, M., Reichert, A.S., Koch, I., Wittig, I., and Brandt, U. (2012). Complexome profiling identifies TMEM126B as a component of the mitochondrial complex I assembly complex. Cell Metab. *16*, 538–549.
30. Pagliarini, D.J., Calvo, S.E., Chang, B., Sheth, S.A., Vafai, S.B., Ong, S.E., Walford, G.A., Sugiana, C., Boneh, A., Chen, W.K., et al. (2008). A mitochondrial protein compendium elucidates complex I disease biology. Cell *134*, 112–123.
31. Carilla-Latorre, S., Gallardo, M.E., Annesley, S.J., Calvo-Garrido, J., Graña, O., Accari, S.L., Smith, P.K., Valencia, A., Garesse, R., Fisher, P.R., and Escalante, R. (2010). MidA is a putative methyltransferase that is required for mitochondrial complex I function. J. Cell Sci. *123*, 1674–1683.
32. Guarani, V., Paulo, J., Zhai, B., Huttlin, E.L., Gygi, S.P., and Harper, J.W. (2014). TIMMDC1/C3orf1 functions as a membrane-embedded mitochondrial complex I assembly factor through association with the MCIA complex. Mol. Cell. Biol. *34*, 847–861.
33. Wessels, H.J., Vogel, R.O., van den Heuvel, L., Smeitink, J.A., Rodenburg, R.J., Nijtmans, L.G., and Farhoud, M.H. (2009). LC-MS/MS as an alternative for SDS-PAGE in blue native analysis of protein complexes. Proteomics *9*, 4221–4228.
34. Wessels, H.J., Vogel, R.O., Lightowlers, R.N., Spelbrink, J.N., Rodenburg, R.J., van den Heuvel, L.P., van Gool, A.J., Gloerich, J., Smeitink, J.A., and Nijtmans, L.G. (2013). Analysis of 953 human proteins from a mitochondrial HEK293 fraction by complexome profiling. PLoS ONE *8*, e68340.
35. Hanein, S., Perrault, I., Roche, O., Gerber, S., Khadom, N., Rio, M., Boddaert, N., Jean-Pierre, M., Brahimi, N., Serre, V., et al. (2009). TMEM126A, encoding a mitochondrial protein, is mutated in autosomal-recessive nonsyndromic optic atrophy. Am. J. Hum. Genet. *84*, 493–498.